

Arrayed waveguide grating near 760 nm wavelength for integrated spectral beam combining applications

Eric J. Stanton, Alexander Spott, Michael L. Davenport, Nicolas Volet, John E. Bowers

Department of Electrical and Computer Engineering, University of California, Santa Barbara, CA 93106, USA

estanton@ece.ucsb.edu

Abstract: An arrayed waveguide grating operating near 760 nm is demonstrated with 0.1 dB insertion loss and -23 dB crosstalk. This device is compatible with a heterogeneously integrated ultra-broadband spectral beam combiner.

OCIS codes: (130.3120) Integrated optics devices; (140.3298) Laser beam combining

1. Introduction

An ultra-broadband spectral beam combiner, fully integrated with light sources, is a desirable technology that would enable advances in spectral sensors, wavelength-division multiplexing (WDM) devices for communications, and high brightness broadband sources. The arrayed waveguide grating (AWG) presented in this work is designed to be compatible with the ultra-broadband (400 nm to 4 μm) integrated spectral beam combiner, Fig. 1(a), described in [1] as an intra-band combining stage.

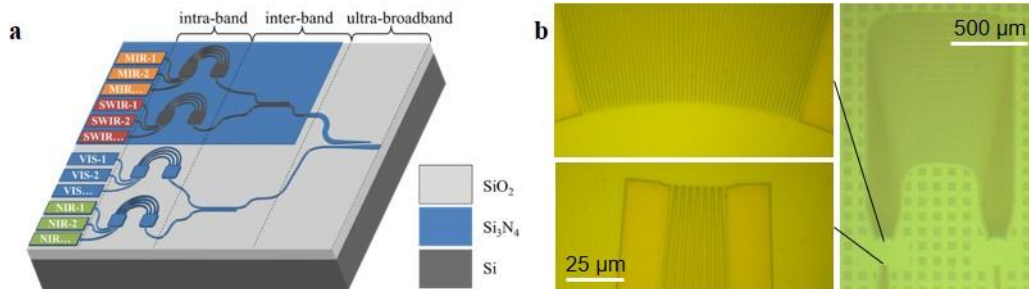


Fig. 1. (a) Integrated spectral beam combining application for this AWG. (b) Micrograph of the fabricated AWG showing detail of the free propagation region interface.

The AWG, shown in Fig. 1(b), is fabricated with Si_3N_4 core and SiO_2 cladding on a silicon substrate, which is compatible with heterogeneously integrated lasers on silicon [2].

While previous AWGs have been demonstrated at visible wavelengths [3,4], those AWGs have reported 5 dB of insertion loss, which makes power scaling not feasible and limits performance for sensor and communication applications. There are several design features in this work to minimize insertion loss and crosstalk. Phase errors and insertion loss are minimized by: 1) eliminating the bend mode mismatch between arrayed waveguides, 2) using a thin core of 60 nm to reduce grating side order excitation while minimizing the number of arrayed waveguides, 3) using the smallest available address unit for writing the lithography mask, and 4) by minimizing the interfacial scattering of the waveguide mode. Finally, hydrogen impurities are minimized from the core and cladding materials to reduce material absorption from molecular bond resonances. These design features minimize the insertion loss, with less than 1 dB demonstrated, and therefore enable integrated spectral beam combining at visible wavelengths.

2. AWG design and fabrication

This AWG is designed as described in [5] with arrayed waveguides having two identical bends, therefore minimizing the phase error caused by varying the bend radius of each arm. This configuration is typically avoided because two extra straight to bend junctions are necessary compared to the configuration with a single bend in each arm. Each bend has a tapered bend radius to minimize this junction loss by dividing each bend into 25 segments of varying radii to adiabatically transition the waveguide from straight to a minimum of radius of 150 μm and back to straight. The thin core of 60 nm reduces grating side mode excitation by narrowing the far field divergence of the waveguides incident at the free propagation region. Scattering loss is minimized by optimizing the lithography and etching processes to reduce the waveguide's sidewall roughness and by maximizing the waveguide width to height ratio for a desired minimum bend radius as discussed in [6]. In this case the waveguide width is 1 μm and height is 60 nm. Simulations show a minimum bend radius of 150 μm has negligible loss on the order of $5 \cdot 10^{-3}$ dB/cm. The waveguide sidewall and surface roughness are measured with an atomic force microscope (AFM) to have a standard

deviations $\sigma_{\text{side}} = 1.3$ nm and $\sigma_{\text{surface}} = 0.8$ nm and correlation lengths $L_{c,\text{side}} = 46.2$ nm and $L_{c,\text{surface}} = 50.8$ nm. Fig. 2(a) shows simulations of interfacial scattering loss, bend loss, and mode indices as a function of waveguide bend curvature, which is the inverse of the radius.

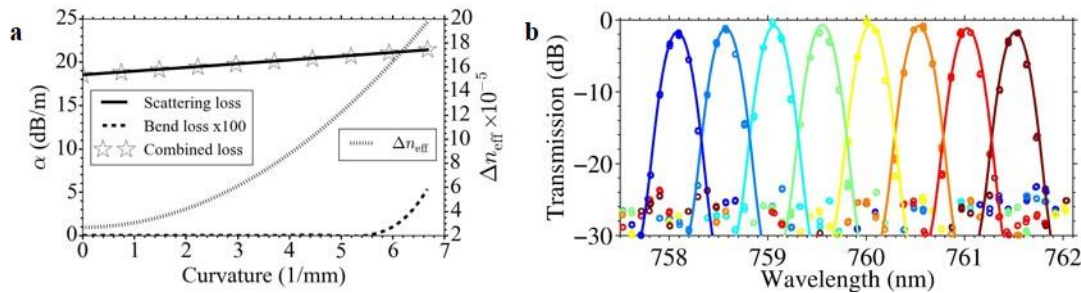


Fig. 2. (a) Scattering and bend losses simulated for a 760 nm wavelength. Also shown is the index shift, Δn_{eff} , from a nominal value of $n_{\text{eff}} = 1.4945$ for all curvature, inverse of the bend radius, in each bend of the arrayed waveguides. (b) Measured transmission spectra (circles) and theoretical calculations (solid lines) for each channel represented by different colors.

Bend modes and radiation losses are calculated with FIMMWAVE commercial software and the interfacial scattering loss is calculated as in [6] using the measured sidewall and surface roughness. Absorption loss due to bond resonances from hydrogen impurities is the dominating absorption loss mechanism for a similar waveguide in [7], where the measured absorption resonances near 1540 nm are second order resonances so the first order resonances would appear near 770 nm. We do not have a method of measuring these first order bond resonance absorption peaks directly, however, the fabrication process for this AWG is designed to reduce the hydrogen impurities to minimize the strength of these bond resonances by baking the wafers at 1050°C for 10 hours before and after the top oxide deposition. Therefore, the combined bend radiation and interfacial scattering loss of 21 dB/m predicts the minimum limit of the total propagation loss since absorption loss is neglected.

Fabrication begins with 100 mm silicon wafers with 2 μm of thermal SiO_2 and 60 nm of Si_3N_4 deposited by low-pressure chemical vapor deposition (LPCVD) from Rogue Valley Microdevices. Deep UV lithography and $\text{CF}_4/\text{CHF}_3/\text{O}_2$ inductively coupled plasma (ICP) etch are used to define the AWG pattern. The SiO_2 top cladding is deposited with plasma enhanced chemical vapor deposition (PECVD). The wafer is then diced and the facets are polished.

3. Experiment and Results

The transmission spectrum of the AWG is measured with a TE polarized tunable laser focused to each demultiplexed waveguide facet with an objective lens and then collected from the multiplexed waveguide facet with a lensed fiber, which is coupled to an optical spectrum analyzer (OSA). The OSA tracks the lasing wavelength peak and integrates a 0.3 nm span for each transmission data point at the laser is tuned to reduce side mode noise. Fig. 2(b) shows the measured transmission spectra and theoretical calculations for each AWG channel. The transmission spectrum of each channel is normalized to the transmission spectrum of a straight waveguide with the same facet geometry. From the normalized transmission spectrum, the channel crosstalk is -23 dB and the insertion loss is 0.1 dB at the peak of the fifth channel, shown in yellow. The non-uniformity is 1.7 dB and the free spectral range (FSR) is 6.9 nm. The theoretical AWG transmission spectrum uses an adjusted modal index, which deviates from the simulated value by 0.05.

Since the insertion loss and crosstalk are low with less than 1 dB insertion loss, this demonstration proves the feasibility of integrated spectral beam combiners and subsequently, integrated technologies for sensing, WDM communication, and high brightness broadband sources operating at visible wavelengths.

We acknowledge support from the U.S. Office of Naval Research (ONR) under Grant No. N00014-13-C-0147 and N. V. acknowledges support from the Swiss National Science Foundation.

- [1] E. J. Stanton *et al.*, "Multi-octave spectral beam combiner on ultra-broadband photonic integrated circuit platform," *Opt. Express* **23**, 11272 (2015).
- [2] J. T. Bovington *et al.*, "Heterogeneous lasers and coupling to Si_3N_4 near 1060 nm," *Opt. Lett.* **39**, 6017 (2014).
- [3] Y. Komai *et al.*, "Compact Spectroscopic Sensor Using a Visible Arrayed Waveguide Grating," *Jpn. J. Appl. Phys.* **45**, 6742 (2006).
- [4] E. Segev *et al.*, "Visible Array Waveguide Gratings for Applications of Optical Neural Probes," *Proc. SPIE* **9305** (2015).
- [5] M. K. Smit and C. van Dam, "PHASAR-based WDM-devices: Principles, design and applications," *IEEE JTSQE* **2**, 236 (1996).
- [6] J. F. Bauters *et al.*, "Ultra-low-loss high-aspect-ratio Si_3N_4 waveguides," *Opt. Express* **19**, 3163 (2011).
- [7] J. F. Bauters *et al.*, "Planar waveguides with less than 0.1 dB/m propagation loss fabricated with wafer bonding," *Opt. Express* **19**, 24090 (2011).